H1prelim-08-111 Submitted to

34th International Conference on High Energy Physics, 30th July- 5th August, 2008, Philadelphia
Parallel Session **QCD**

Electronic Access:https://www-h1.desy.de/publications/H1preliminary.short_list.html

Leading Neutron production in DIS at HERA

H1 Collaboration

Abstract

The production of highly energetic forward neutrons has been studied in deep-inelastic positron-proton scattering. The data were taken with the H1 detector at HERA in the years 2006-2007 and correspond to an integrated luminosity of 122 pb^{-1}. Semi-inclusive cross sections have been measured in the range of four momentum transfer squared $6 < Q^2 < 100\ \mathrm{GeV}^2$, Bjorken scaling variable $1.5 \cdot 10^{-4} < x < 3 \cdot 10^{-2}$ and the fractional momentum of the neutron $0.32 < x_L < 0.95$. The data are used to estimate the structure function of the pion.

1 Introduction

Hadronic correlations in the proton in form of virtual pions are believed to play an important dynamical role in the nucleon structure. The proton might fluctuate into a state consisting of a pion and a neutron ($p \to n\pi^+$). Numerous theoretical works have suggested, that the production of highly energetic, forward neutrons in deep-inelastic ep scattering is sensitive to the structure of pion for which our knowledge from fixed target experiments is limited to high x values.

Here, we report the measurement of the semi–inclusive cross sections for leading neutron production in deep–inelastic scattering (DIS) in the reaction $ep \to enX$. The data were taken during 2006-2007 using the HERA accelerator at DESY where 27.5 GeV positrons collided with 920 GeV protons. The total luminosity of the sample used in this analysis is $122\ \mathrm{pb}^{-1}$.

We use the kinematic variables x, Q^2 and y to describe the inclusive DIS scattering process. They are defined as:

$$x = \frac{-q^2}{2p\cdot q} \qquad Q^2 = -q^2 \qquad y = \frac{p\cdot q}{p\cdot k}\ , \tag{1}$$

where p, k and q are the four–momenta of the incident proton, the incident positron and the exchanged virtual photon coupling to the positron. At the ep center–of–mass energy $\sqrt{s}$ they are related by $Q^2 = sxy$.

The kinematic variables used to describe a final state neutron are:

$$t = (p-p')^2 \simeq -\frac{p_T^2}{x_L} - (1-x_L)\left(\frac{m_n^2}{x_L} - m_p^2\right) \qquad x_L = 1 - \frac{q\cdot(p-p')}{q\cdot p} \simeq E'/E_p, \tag{2}$$

where p' is the four–momentum of the final state neutron, m_n is the mass of the neutron and m_p is the proton mass. As defined, t corresponds to the squared four–momentum transferred between the incident proton and the final state neutron.

The four–fold differential cross section for baryon production can be parameterised by a semi–inclusive structure function, $\mathrm{F}_2^{\mathrm{LN}(4)}$, defined by:

$$\frac{\mathrm{d}^4\sigma(ep\to enX)}{\mathrm{d}x\,\mathrm{d}Q^2\,\mathrm{d}x_L\,\mathrm{d}t} = \frac{4\pi\alpha^2}{x\,Q^4}\left(1 - y + \frac{y^2}{2}\right)\mathrm{F}_2^{\mathrm{LN}(4)}(x, Q^2, x_L, t), \tag{3}$$

The four–fold differential cross section integrated over $0 \le p_T \le 200$ MeV defines the semi–inclusive structure function $\mathrm{F}_2^{\mathrm{LN}(3)}$ which we measure:

$$\begin{aligned}\frac{\mathrm{d}^3\sigma(ep\to enX)}{\mathrm{d}x\,\mathrm{d}Q^2\,\mathrm{d}x_L} &= \int_{t_0}^{t_{\min}} \frac{4\pi\alpha^2}{x\,Q^4}\left(1 - y + \frac{y^2}{2}\right)\mathrm{F}_2^{\mathrm{LN}(4)}(x, Q^2, x_L, t)\,\mathrm{d}t \\ &= \frac{4\pi\alpha^2}{x\,Q^4}\left(1 - y + \frac{y^2}{2}\right)\mathrm{F}_2^{\mathrm{LN}(3)}(x, Q^2, x_L),\end{aligned} \tag{4}$$

where the integration limits are:

$$t_{\min} = -(1-x_L)\left(\frac{m_n^2}{x_L} - m_p^2\right) \qquad t_0 = -\frac{(200\,\mathrm{MeV})^2}{x_L} + t_{\min}. \tag{5}$$

2 Event selection

The analysis uses the data sample collected in positron-proton interactions in 2006-2007. Events were triggered by combinations of the SPACAL electron and the Forward Neutron Calorimeter (FNC) triggers. The trigger efficiency is close to 100%. The total integrated luminosity of the data sample is $122\ \mathrm{pb}^{-1}$.

Further cuts are applied to ensure the quality of the data and to remove non-DIS events: the event vertex is required to be within 35 cm of the nominal interaction point. The energy and the angle of scattered electron are required to be $E_e > 11$ GeV and $156^\circ < \theta_e < 175^\circ$, respectively. Furthermore, events are selected within the DIS kinematic ranges $6 < Q^2 < 100\ \mathrm{GeV}^2$, $0.02 < y < 0.6$ and $1.5 \cdot 10^{-4} < x < 0.3 \cdot 10^{-1}$.

Events containing a leading neutron are selected by requiring a neutral hadronic cluster in the FNC with an energy above 300 GeV and a polar angle below 0.75 mrad. The acceptance of the FNC is defined by the aperture of the HERA beamline magnets and is about 30% for the neutrons in the choosen angular range.

About 300,000 events are selected which satisfy all selection cuts.

3 Monte Carlo Models

Monte Carlo samples have been used to correct the data for inefficiencies, acceptances and resolution effects of the detector components and for effects of QED radiation.

The RAPGAP 3.1 program is used to generate the pion exchange process. In this model, the incident proton is splitted into a neutron and a π^+, which then undergoes a DIS interaction.

The cross-section of electron–proton scattering takes the form

$$d\sigma(ep \to nX) = f_{\pi^+/p}(x_L, t) \cdot d\sigma(e\pi^+ \to X) \tag{6}$$

where $f_{\pi^+/p}(x_L, t)$ represents the pion flux associated with the beam proton and $d\sigma(ep\pi^+ \to X)$ is the cross section of the electron–pion interaction. The pion flux factor is taken from the light-cone representation of Holtmann et al. [2].

$$f_{\pi^+/p}(x_L, t) = \frac{1}{2\pi}\frac{g^2_{p\pi N}}{4\pi}(1 - x_L)\frac{-t}{(m_\pi^2 - t)^2}\exp\left(-R^2_{\pi n}\frac{m_\pi^2 - t}{1 - x_L}\right) \tag{7}$$

where m_π is a pion mass, $g^2_{p\pi^+ n}/4\pi = 13.6$ is the $p\pi n$ coupling constant known from phenomenological analyses of low-energy data, $R_{\pi n} = 0.93\ \mathrm{GeV}^{-1}$ is the radius of pion-proton Fock state [2].

The program DJANGOH 14 generates complete events in DIS. It is based on leading order electroweak cross sections and takes QCD effects to order α_s into account.

4 Results

Figure 1 shows the the neutron energy and the transverse momentum distributions observed from the DIS interactions, compared with the Monte Carlo simulation.

The semi-inclusive structure function $F_2^{LN}(Q^2, x, x_L)$ is measured in 7 bins in Q^2, 7 bins in x and 7 bins in x_L in the ranges $6 < Q^2 < 100$ GeV^2, $1.5 \cdot 10^{-4} < x < 3 \cdot 10^{-2}$ and $0.32 < x_L < 0.95$. Figure 2 shows the results of $F_2^{LN}(Q^2, x, x_L)$. The measurements are compared with the predictions of the DJANGO and RAPGAP Monte Carlo models. Apparently, the standard DIS Monte Carlo simulation DJANGO doesn't describe the distributions, in particular at higher x_L values. On the other hand, this region is well described by the pion exchange Monte Carlo program RAPGAP, giving the support to the hypothesis that at high x_L the dominant mechanism for leading neutron production is the pion exchange. The best description of the data is achieved if the predictions of the RAPGAP (with pion exchange) and the DJANGO Monte Carlo programs are summed with some weighting factors (0.64 × RAPGAP + 1.23 × DJANGO). The comparison can be seen in detail in the Figure 4 where the $F_2^{LN}(Q^2, x, x_L)$ is shown in one selected (x, Q^2) bin.

In the Figure 5 the ratios of the measured semi-inclusive structure function $F_2^{LN}(Q^2, x, x_L)$ to the inclusive F_2 structure functions are shown in (x, Q^2) bins. The values of F_2 are obtained from the H1-2000 parameterisation of the parton density [1]. The ratios are almost flat in all (x, Q^2) bins implying that the F_2^{LN} and F_2 have a similar (x, Q^2) behavior. This result suggests the validity of factorization i.e. independence of the photon and the proton vertices. An overall suppression of leading neutron production, however, predicted by some theoretical analyses is still possible.

Based on the assumption that at high x_L the leading neutron production is dominated by the pion exchange mechanism, the measurement of F_2^{LN} can provide an important information about the pion structure. The quark and gluon distributions of the pion have previously been constrained using Drell–Yan data and direct photon production data obtained by πp scattering experiments and are limited to high x ($x \gtrsim 0.1$) values.

We use the measurement of $\mathrm{F}_2^{\mathrm{LN(3)}}$ at $0.68 < x_L < 0.77$ and the integral of the pion flux factor to estimate the pion structure function at low Bjorken–x. Assuming that the Regge model of leading neutron production is valid, the quantity $\mathrm{F}_2^{\mathrm{LN(3)}}/\Gamma_\pi$ can be associated to the structure function of the pion where:

$$\Gamma_\pi(x_L = 0.73) = \int_{t_0}^{t_{\min}} f_{\pi/p}(x_L = 0.73, t)\,\mathrm{d}t = 0.131. \tag{8}$$

Figure 6 shows $\mathrm{F}_2^{\mathrm{LN(3)}}/\Gamma_\pi$ as a function of Q^2 for fixed values of β and Figure 7 shows $\mathrm{F}_2^{\mathrm{LN(3)}}/\Gamma_\pi$ as a function of β for fixed values of Q^2. The data are compared to predictions of parameterisations of the pion structure function [4, 5]. The measurements are also compared to the H1-2000 parameterisation of the proton structure function [1] which is multiplied by the factor 2/3 according to naive expectation based on the number of valence quarks in the pion and proton respectively.

The Q^2 distribution exhibits the rise with Q^2 (i.e. scaling violation) for higher β, and the β distributions show a steep rise with decreasing β, in accordance with the pion and the proton structure function parameterisations. It should be noted, that there exist also other parameterisations of the pion structure function which show much flatter behavior as function of β and which were ruled out by the previous H1 and ZEUS measurements [6, 7].

In absolute values, the presented data are slightly below the expectations, suggesting that additional phenomena, like absorption, may play a role. It should be noted, that the evaluation of the pion flux factor used here is not without some theoretical uncertainty. Setting the exponential term (formfactor) of eq.7 to 1.0 yields a pion flux of $\Gamma_\pi = 0.203$, instead of 0.131, which however would imply even larger absorption effects.

5 Summary

The production of highly energetic forward neutrons has been studied in deep-inelastic positron-proton scattering. The semi–inclusive cross section $ep \rightarrow enX$ has been measured in the kinematic region $6 \leq Q^2 \leq 100$ GeV^2, $1.5 \cdot 10^{-4} \leq x \leq 3 \cdot 10^{-2}$, $0.32 < x_L < 0.95$ and $p_T^n \leq 200$ MeV.

The semi–inclusive cross sections for leading neutrons with $x_L \gtrsim 0.7$ can be described entirely by the π^+ exchange model. The semi-inclusive structure function F_2^{LN} and the inclusive structure function F_2 have similar (x, Q^2) behavior, supporting vertex factorisation.

The data are used to estimate the structure function of the pion.

References

[1] H1 Collab., C. Adloff et al., *Eur. Phys. J.* **C21** (2001) 33.

[2] H. Holtmann et al., *Phys.Lett.* **B338** (1994) 363.

[3] M. Bishari, *Phys.Lett.* **B38** (1972) 510.

[4] M. Glück, E. Reya and I. Schienbein, *Eur.Phys.J.* **C10** (1999) 313-317.

[5] P. Aurenche et al., *Phys. Lett.* **B233** (1989) 517.

[6] H1 Collab., C. Adloff et al., *Eur. Phys. J.* **C6** (1999) 587.

[7] ZEUS Collab., S.Chekanov., *Nucl. Phys.* **B637** (2002) 3.

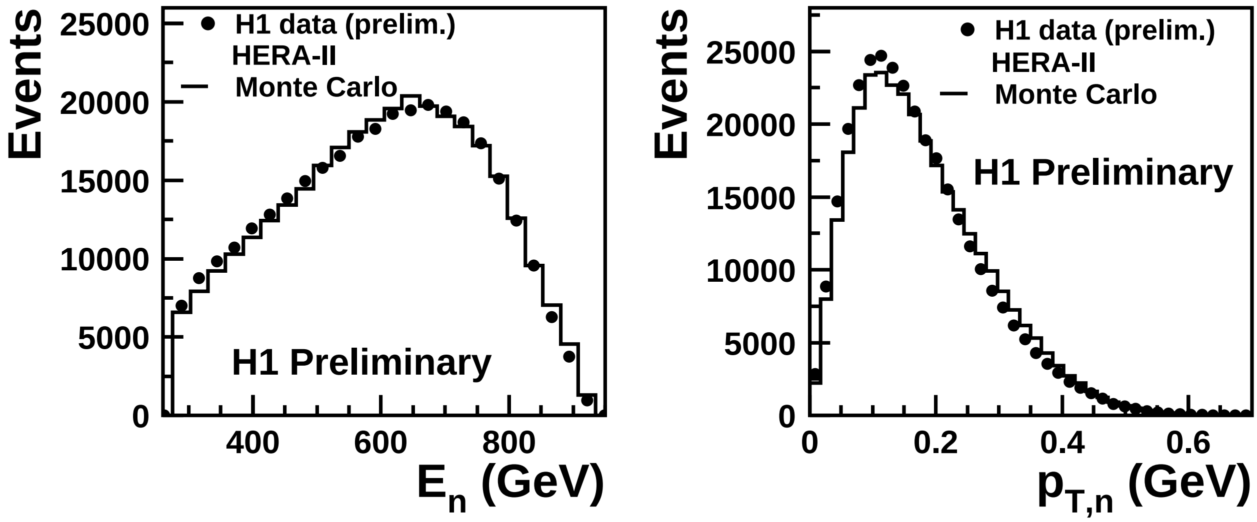

Figure 1: The observed neutron energy spectrum and the transverse momentum p_T distribution from the DIS interactions. The data distribution is compared with the Monte Carlo simulation, which is the mixture of RAPGAP with pion exchange and the DJANGO models ($0.64\times$ RAPGAP$+1.23\times$DJANGO).

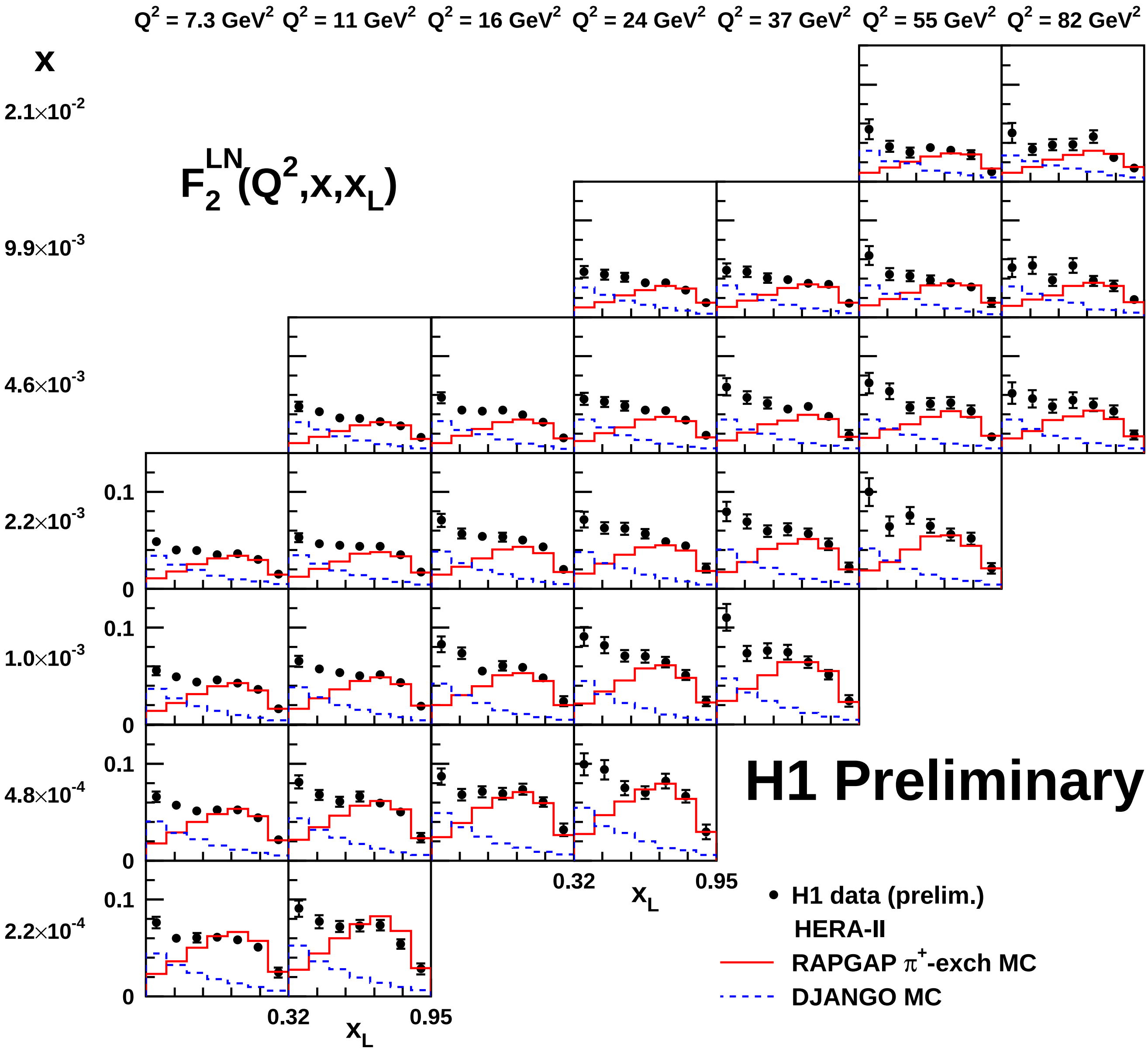

Figure 2: The semi–inclusive structure function $F_2^{LN(3)}$, for neutrons with $p_T \leq 200$ MeV, compared to the predictions of the DJANGO and RAPGAP Monte Carlo models calculated using GRV leading order parton distributions for the proton and the pion respectively.

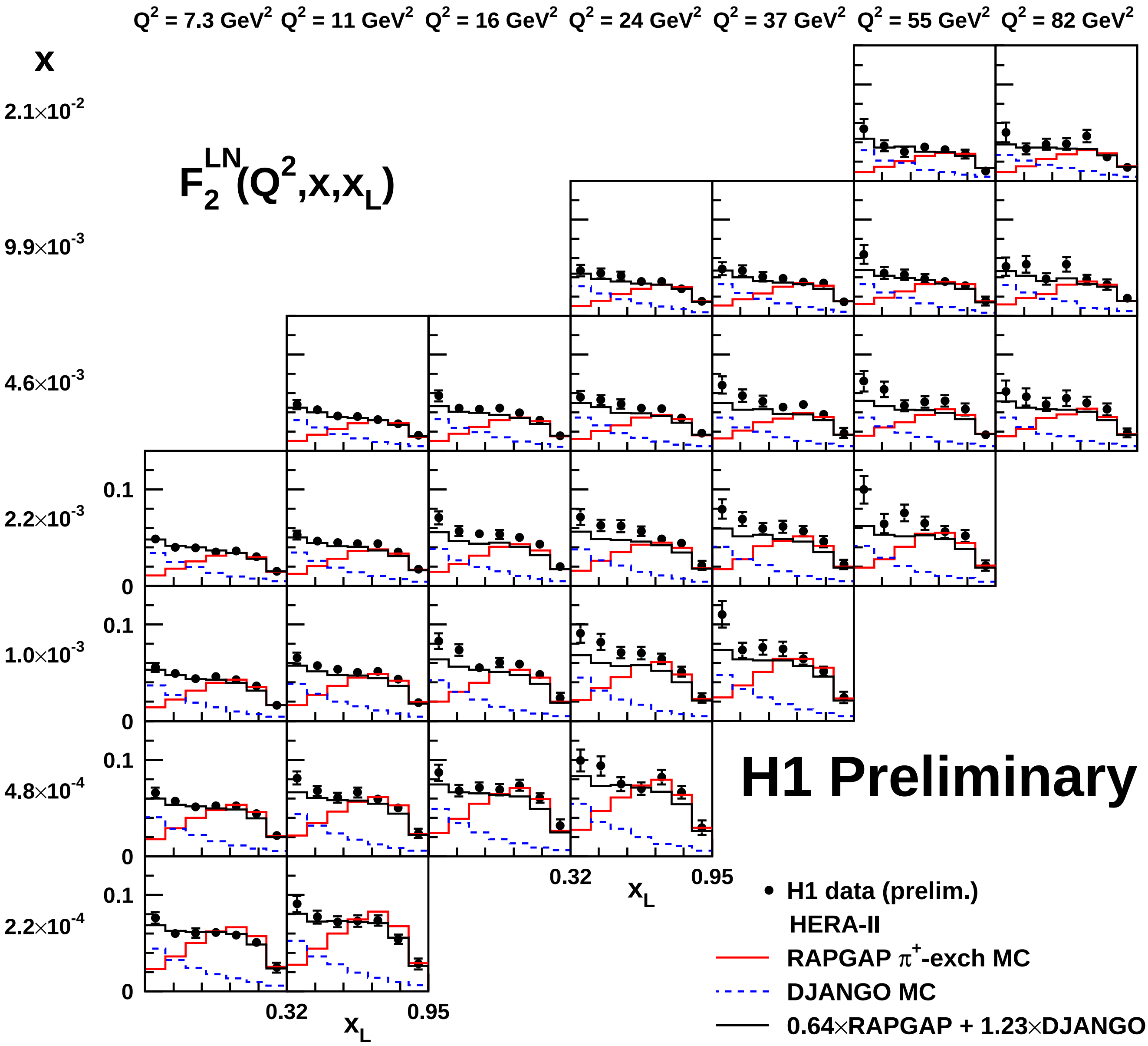

Figure 3: The semi–inclusive structure function $F_2^{LN(3)}$, for neutrons with $p_T \leq 200$ MeV, compared to the predictions of the DJANGO and RAPGAP Monte Carlo models calculated using GRV leading order parton distributions for the proton and the pion respectively. The full line represents the weighted sum of RAPGAP and DJANGO model predictions.

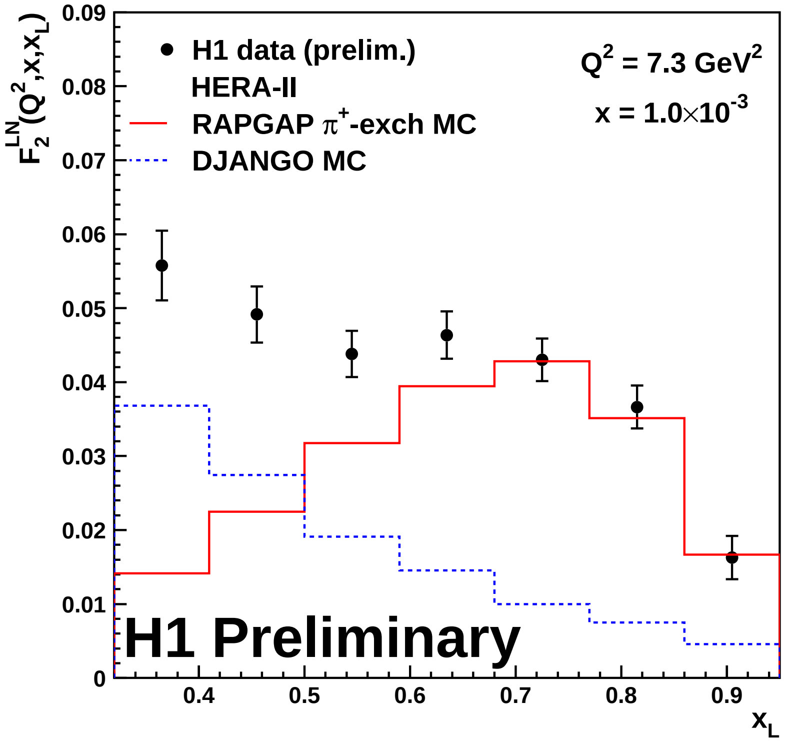

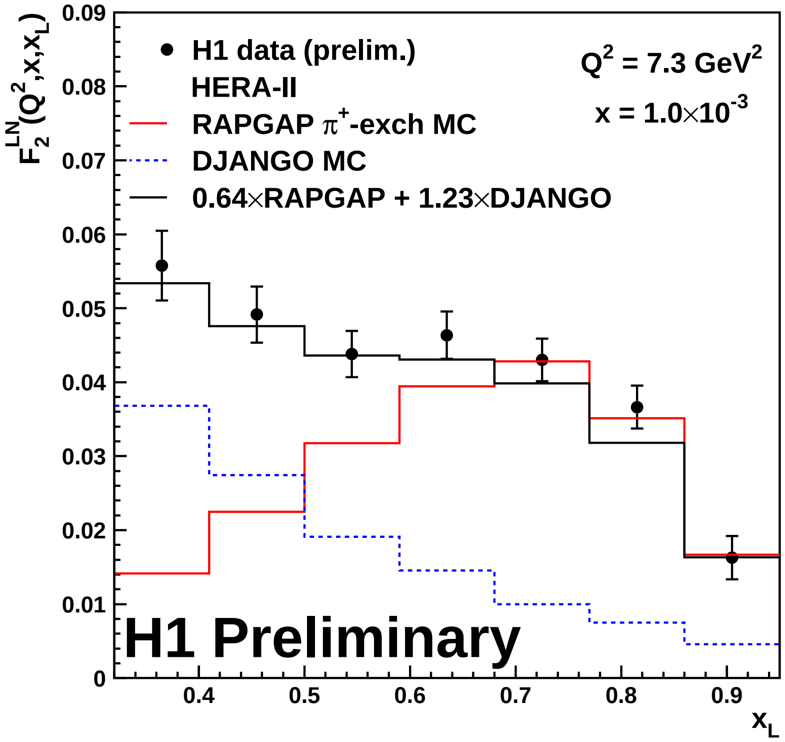

Figure 4: The semi–inclusive structure function $\mathrm{F}_2^{\mathrm{LN}(3)}$, for neutrons with $p_T \leq 200$ MeV, compared to the predictions of the DJANGO and RAPGAP Monte Carlo models calculated using GRV leading order parton distributions for the proton and the pion respectively. One (Q^2,x)-bin is shown in detail. In the lower plot, the full line represents the weighted sum of RAPGAP and DJANGO model predictions.

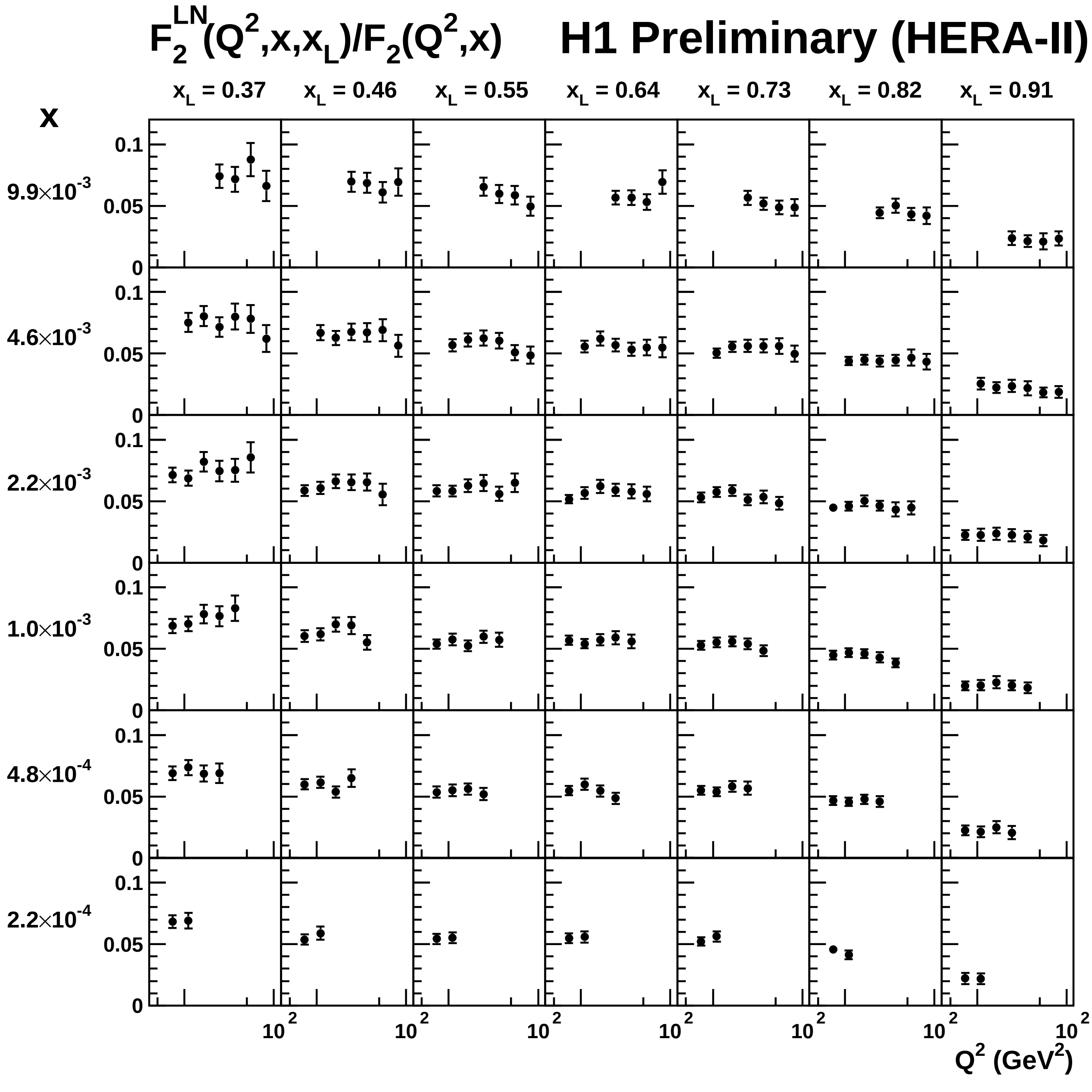

Figure 5: The ratio of the semi–inclusive structure function $\mathrm{F}_2^{\mathrm{LN}(3)}$, for neutrons with $p_T \leq$ 200 MeV, to the inclusive structure function F_2 obtained from the H1 measurements [1] of deep-inelastic scattering.

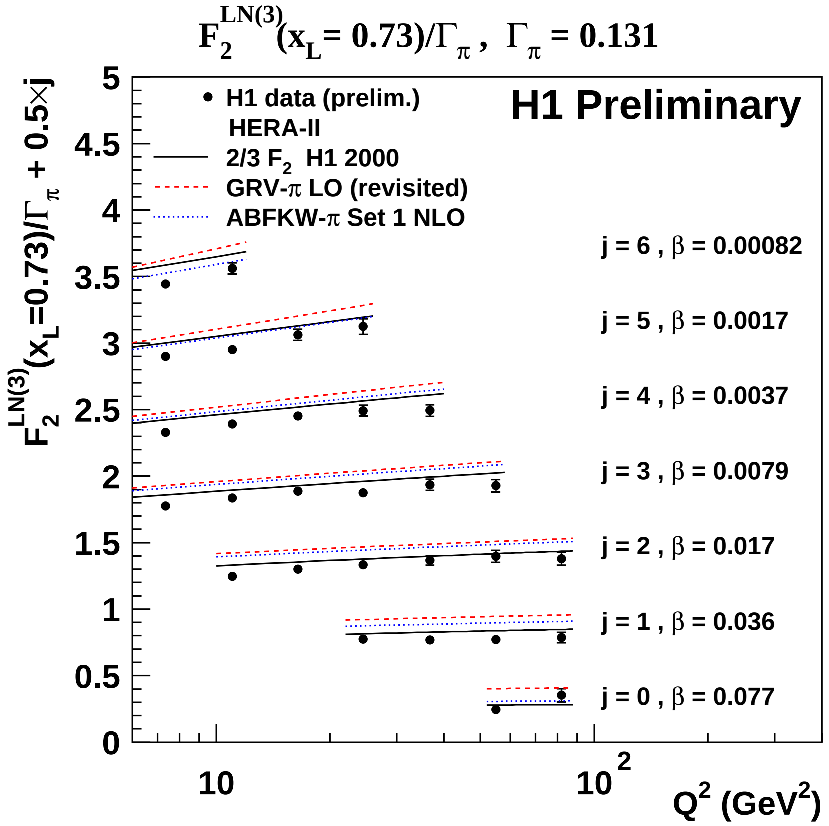

Figure 6: $F_2^{LN(3)}/\Gamma_\pi$ at $x_L = 0.73$ plotted as a function of Q^2 for fixed values of β. The quantity Γ_π is the p_T integrated pion flux factor. The pion flux is defined by eq.9, where m_π is the pion mass, $g^2_{p\pi n}/4\pi = 13.6$ is the $p\pi n$ coupling constant and $R_{\pi n} = 0.93$ GeV^{-1} is the radius of the pion-proton Fock state [2].

$$f_{\pi^+/p}(x_L, t) = \frac{1}{2\pi}\frac{g^2_{p\pi N}}{4\pi}(1 - x_L)\frac{-t}{(m_\pi^2 - t)^2}\exp\left(-R^2_{\pi n}\frac{m_\pi^2 - t}{1 - x_L}\right) \tag{9}$$

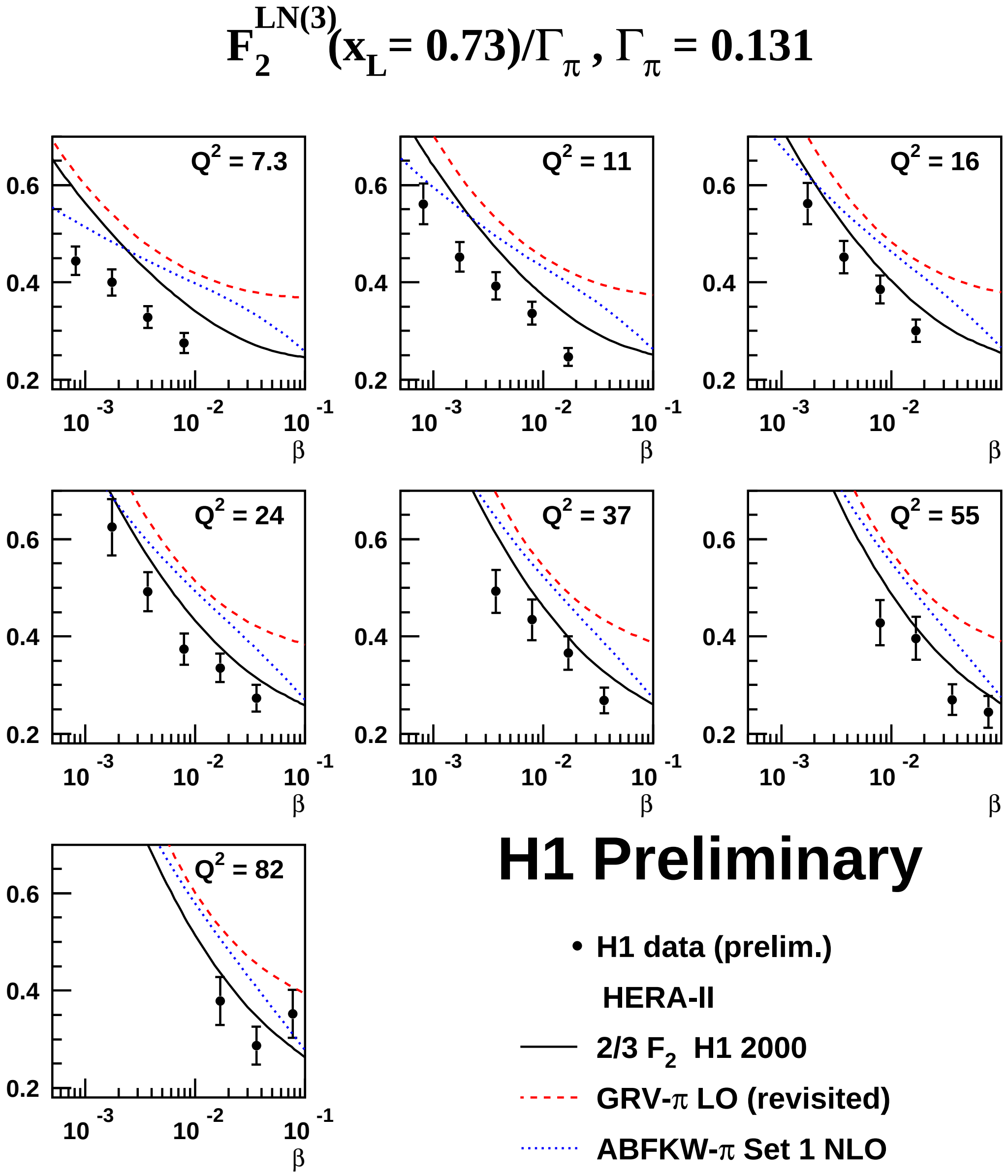

Figure 7: $\mathrm{F}_2^{\mathrm{LN(3)}}/\Gamma_\pi$ at $x_L = 0.73$ plotted as a function of β for fixed values of Q^2. The quantity Γ_π is the p_T integrated pion flux factor. The pion flux is defined by eq.9 (see caption of Fig.6).